COMMUNICATIONS IN NUMERICAL METHODS IN ENGINEERING
Commun. Numer. Meth. Engng 2000; **00**:1–6 *Prepared using* cnmauth.cls *[Version: 2000/03/22 v1.0]*

Discontinuous Galerkin methods for flow and transport problems in porous media

Béatrive Rivière *and Mary F. Wheeler

The Center for Subsurface Modeling, Texas Institute for Computational and Applied Mathematics, The University of Texas at Austin, ACE 5.332, 201 East 24th Street, Austin TX 78712

SUMMARY

This work presents a new scheme based on discontinuous approximation spaces for solving the miscible displacement problem in porous media. Numerical comparisons are made between this scheme and the well known mixed finite element and higher order Godunov methods. The simulations clearly show the advantages of the discontinuous Galerkin methods for stable or unstable flow. Copyright © 2000 John Wiley & Sons, Ltd.

KEY WORDS: miscible displacement, higher order schemes, discontinuous polynomials, unstructured meshes, unstable flow

1. Introduction

We consider the displacement of one incompressible fluid by another in a porous medium Ω in $\mathbb{R}^2$. The invading and the displaced fluids are referred to as the solvent and the resident fluid; respectively. Let J denote the time interval $(0, T_f]$. The classical equations governing the miscible displacement in Ω over J are:

$$\begin{aligned} -\nabla \cdot \left(\frac{K}{\mu(c)} \nabla p\right) &\equiv \nabla \cdot \boldsymbol{u} = 0, \qquad \text{in} \quad \Omega \times J, \\ \phi \frac{\partial c}{\partial t} + \nabla \cdot (\boldsymbol{u} c - \boldsymbol{D}(\boldsymbol{u}) \nabla c) &= R(c), \qquad \text{in} \quad \Omega \times J, \end{aligned}$$

where the dependent variables are p, the pressure in the fluid mixture, and c, the fraction volume of the solvent in the fluid mixture. The permeability K of the medium measures the resistance of the medium to fluid flow; μ is the viscosity of the fluid mixture; $\boldsymbol{u}$ represents the Darcy velocity, ϕ is the porosity of the medium and $\boldsymbol{D}(\boldsymbol{u})$ is the coefficient of molecular diffusion and mechanical dispersion that depends on $\boldsymbol{u}$ in a nonlinear fashion. A survey on simulating miscible displacement can be found in [3].

The boundary of the domain is decomposed into a Dirichlet part Γ_D and a Neumann part Γ_N such that $\Gamma_D \cap \Gamma_N = \emptyset$ and $\overline{\Gamma_D \cup \Gamma_N} = \partial\Omega$. We also define the inflow part $\Gamma_- \equiv \{\boldsymbol{x} \in \partial\Omega : \boldsymbol{u} \cdot \boldsymbol{\nu} < 0\}$

*Correspondence to: The Center for Subsurface Modeling, Texas Institute for Computational and Applied Mathematics, The University of Texas at Austin, ACE 5.332, 201 East 24th Street, Austin TX 78712

and the outflow part $\Gamma_+ \equiv \{\boldsymbol{x} \in \partial\Omega : \boldsymbol{u}\cdot\boldsymbol{\nu} \geq 0\}$, where $\boldsymbol{\nu}$ denotes the unit outward normal vector to $\partial\Omega$. We assume Dirichlet and Neumann boundary conditions for the pressure and Neumann and mixed boundary conditions for the concentration. The viscosity of the fluid mixture is assumed to follow the quarter-power mixing law, commonly applicable to hydrocarbon mixtures [5]: $\mu(c) = (c\mu_s^{-0.25} + (1-c)\mu_o^{-0.25})^{-4}$ where μ_s (resp. μ_o) is the viscosity of the solvent (resp. resident fluid). The stability of the flow is characterized by the mobility ratio, i.e. the ratio of the viscosity of the resident fluid to the viscosity of the solvent. Instabilities in the flow will grow if the mobility ratio is larger than unity. In that case, protusions referred to as viscous fingering develop through the resident fluid. Another important physical parameter is the Peclet number that quantifies the convective effects with respect to the dispersive effects.

2. Notation and scheme

Let $\mathcal{E}_h^F = \left\{E_1^F, E_2^F, \ldots, E_{N_h^F}^F\right\}$ and $\mathcal{E}_h^T = \left\{E_1^T, E_2^T, \ldots, E_{N_h^T}^T\right\}$ be two non-degenerate subdivisions of Ω, that consist of triangles or quadrilaterals . The edges of $\mathcal{E}_h^F$ (resp. $\mathcal{E}_h^T$) are denoted by e_k^F (resp. e_k^T). Let P_h^F (resp. P_h^T) denote the number of interior edges in $\mathcal{E}_h^F$ (resp. $\mathcal{E}_h^T$). On each edge e_k^F (resp. e_k^T), a unit normal vector $\boldsymbol{\nu}_k^F$ (resp. $\boldsymbol{\nu}_k^T$) is arbitrarily fixed, except on the boundary $\partial\Omega$ where it coincides with the outward unit normal vector. The direction of $\boldsymbol{\nu}_k^F$ uniquely defines the jump of the function ϕ: $[\phi] = \phi|_{E_1} - \phi|_{E_2}$ if $\boldsymbol{\nu}_k^F$ is from E_1 to E_2. The average of ϕ is defined by $\{\phi\} = (\phi|_{E_1} + \phi|_{E_2})/2$. For r^F and r^T positive integers, one defines the following discrete spaces

$$\mathcal{D}_{r^F}(\mathcal{E}_h^F) = \{v : v|_{E_j^F} \in P_{r^F}(E_j^F),\ \forall j\}, \quad \mathcal{D}_{r^T}(\mathcal{E}_h^T) = \{v : v|_{E_j^T} \in P_{r^T}(E_j^T),\ \forall j\}.$$

We now formally define two bilinear forms.

$$\begin{aligned}
a_{NS}(c;p,v) &= \sum_{j=1}^{N_h^F}\int_{E_j^F}\frac{K}{\mu(c)}\nabla p\nabla v - \sum_{k=1}^{P_h^F}\int_{e_k^F}\{\frac{K}{\mu(c)}\nabla p\cdot\boldsymbol{\nu}_k^F\}[v] + \sum_{k=1}^{P_h^F}\int_{e_k^F}\{\frac{K}{\mu(c)}\nabla v\cdot\boldsymbol{\nu}_k^F\}[p]\\
&\quad - \sum_{e_k^F\in\Gamma_D}\int_{e_k^F}(\frac{K}{\mu(c)}\nabla p\cdot\boldsymbol{\nu}_k^F)v + \sum_{e_k^F\in\Gamma_D}\int_{e_k^F}(\frac{K}{\mu(c)}\nabla v\cdot\boldsymbol{\nu}_k^F)p,\\
b_{NS}(\boldsymbol{u};c,w) &= \sum_{j=1}^{N_h^T}\int_{E_j^T}\boldsymbol{D}(\boldsymbol{u})\nabla c\nabla w - \int_{E_j^T} c\boldsymbol{u}\cdot\nabla w + \sum_{k=1}^{P_h^T}\int_{e_k^T} c^*\boldsymbol{u}\cdot\boldsymbol{\nu}_k^T[w]\\
&\quad + \sum_{e_k^T\in\Gamma_+}\int_{e_k^T} c\boldsymbol{u}\cdot\boldsymbol{\nu}_k^T w - \sum_{k=1}^{P_h^T}\int_{e_k^T}\{\boldsymbol{D}(\boldsymbol{u})\nabla c\cdot\boldsymbol{\nu}_k^T\}[w] + \sum_{k=1}^{P_h^T}\int_{e_k^T}\{\boldsymbol{D}(\boldsymbol{u})\nabla w\cdot\boldsymbol{\nu}_k^T\}[c].
\end{aligned}$$

where c^* is the upwind value of the concentration on a given edge. We also define the functionals

$$L_F(v) = \sum_{e_k^F\in\Gamma_D}\int_{e_k^F}(\frac{K}{\mu(c)}\nabla v\cdot\boldsymbol{\nu}_k^T)p_0, \quad L_T(w) = \int_\Omega R(c)w - \sum_{e_k^T\in\Gamma_-}\int_{e_k^T} c_{\mathrm{in}}\boldsymbol{u}\cdot\boldsymbol{\nu}_k^T w,$$

where p_0 is the Dirichlet datum for pressure and c_{in} is the inflow datum for concentration. The continuous in time Discontinuous Galerkin (DG) [6] method is given by the map $(P^{\mathrm{DG}}, C^{\mathrm{DG}})$:

$[0,T] \to \mathcal{D}_{r^F}(\mathcal{E}_h^F) \times \mathcal{D}_{r^T}(\mathcal{E}_h^T)$ determined by the relations for any t in J

$$a_{NS}(C^{\mathrm{DG}}(t); P^{\mathrm{DG}}(t), v) = L_F(v), \quad \forall\, v \in \mathcal{D}_{r^F}(\mathcal{E}_h^F), \tag{1}$$

$$\int_\Omega \phi \frac{\partial C^{\mathrm{DG}}}{\partial t} w + b_{NS}(\mathbf{U}^{\mathrm{DG}}(t); C^{\mathrm{DG}}, w) = L_T(w), \quad \forall\, w \in \mathcal{D}_{r^T}(\mathcal{E}_h^T). \tag{2}$$

The initial concentration $C^{\mathrm{DG}}(0)$ is the L^2 projection of the initial concentration and the Darcy velocity is defined by $\mathbf{U}^{\mathrm{DG}} = -(K/\mu(C^{\mathrm{DG}}))\nabla P^{\mathrm{DG}}$. We propose a time-stepping procedure that reflects the fact that the velocity field varies more slowly in time than the concentration for reasonable physical data. Thus, the pressure time step $\Delta t_F > 0$ will be chosen to be m times larger than the concentration time step $\Delta t_T > 0$. The procedure has been shown to be efficient for other finite element methods applied to the miscible displacement problem [4]. We denote $t_T^i = i\Delta t_T$ and $t_F^j = j\Delta t_F$. We now describe the algorithm for advancing of one pressure time step. We assume that $t_T^i = t_F^j$ for some fixed indices i and j and that the approximation $C^{\mathrm{DG}}(t_T^i)$ is known. Then, the pressure at time t_F^j can be calculated as the solution of (1) for $t = t_T^i$. The discretization in time of the concentration equation for $t_T^{i+\kappa}$, where $1 \leq \kappa \leq m$, is accomplished by deriving a modified version of the standard backward-difference scheme procedure

$$\int_\Omega \phi \frac{C^{\mathrm{DG}}(t_T^{i+\kappa}) - C^{\mathrm{DG}}(t_T^{i+\kappa-1})}{\Delta t_T} w + b_{NS}(\mathbf{U}_\kappa^{\mathrm{DG}}; C^{\mathrm{DG}}(t_T^{i+\kappa}), w) = L_T(w), \quad \forall\, w \in \mathcal{D}_{r^T}(\mathcal{E}_h^T),$$

where $\mathbf{U}_\kappa^{\mathrm{DG}}$ is a linear extrapolation of $\mathbf{U}^{\mathrm{DG}}(t_F^j)$ and $\mathbf{U}^{\mathrm{DG}}(t_F^{j-1})$. For the first pressure step, this extrapolation is not valid and we use a predictor-corrector technique. The use of slope limiters [2] is also needed to prevent from numerical overshoots and undershoots to occur in the neighborhood of the concentration front.

3. Numerical Experiments

In all experiments, the permeability field is randomly generated on the coarse mesh. We solve for quadratic approximations of the pressure and the concentration.

We first consider the case where both flow and transport equations are solved on structured meshes. In that case, we compare our simulations with those obtained from the Parallel Subsurface Simulator (Parssim) developed at the University of Texas at Austin [1]. In Parssim, flow is simulated using the mixed finite element method and transport is simulated using a higher order Godunov method. Figure 1 shows the permeability field and the concentration front obtained with the DG method in the case of mobility ratio 1 and a low Peclet number. The iscontours $c = 0.25$ obtained with DG and Parssim for low and high Peclet number are shown in Fig. 2. The legend “DG h0-h1” means that flow is solved on the coarse mesh and transport is solved on the mesh refined once. The DG concentration fronts are comparable to those obtained by Parssim even though coarser meshes have been used for DG. We also note that DG velocities are accurate enough to be computed on a coarser mesh than DG concentrations. As we increase the mobility ratio (see Fig. 3), instabilities in the flow yield more fingers in the concentration front. We also observe that DG velocities computed on the coarse mesh produce a much more detailed concentration front than Parssim velocities computed on the coarse mesh.

We then consider the case where flow is solved on an unstructured mesh and transport is solved on a structured mesh. The motivation for solving each equation on a different mesh lies in the fact that in realistic media, the permeability field varies greatly in space in a very unstructured manner. However,

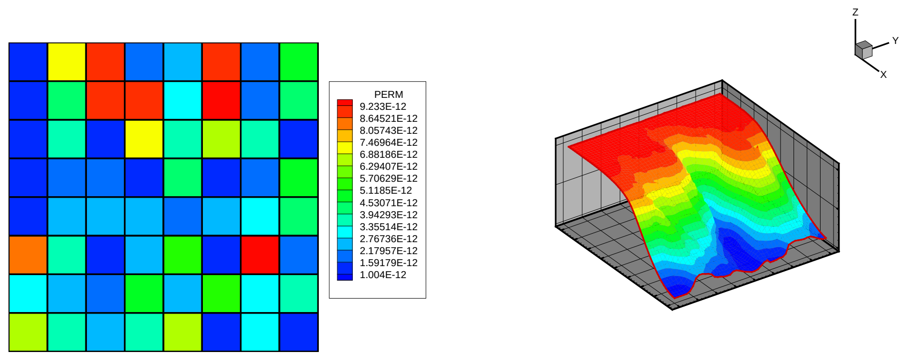

(a) (b)

Figure 1: (a) Permeability field on coarse mesh. (b) DG Concentration front on mesh refined twice for mobility ratio 1 and Peclet number 40.

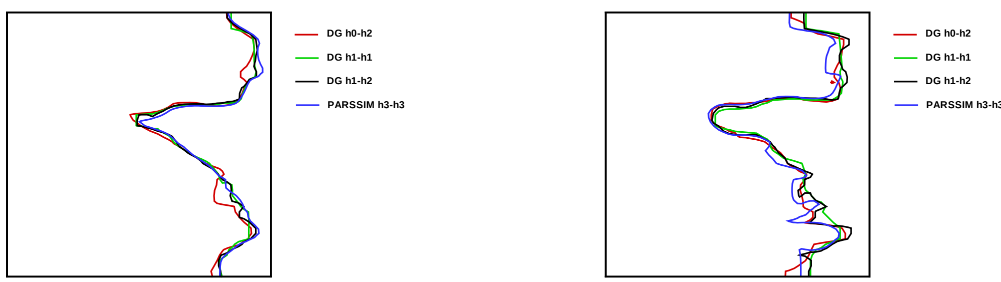

(a) (b)

Figure 2: Comparisons between DG and Parssim concentration isocontours for mobility ratio 1 and Peclet number (a) 40 and (b) 1600.

the porosity of the medium is assumed to be uniform, and structured meshes are prefered for solving the concentration equation. Comparisons with Parssim are not possible since Parssim does not handle unstructured meshes. Figure 4 shows the permeability field and the pressure field obtained in the case of mobility ratio 1. We compare our numerical results to the DG solution computed on the mesh refined twice for both pressure and concentration, which we refer to as the *fine* solution. As the meshes for concentration and pressure are successively refined, we observe that the isocontours converge to the *fine* solution (see Fig. 5 (a)). In the case of high Peclet number, the front has more protusions (see Fig. 5 (b)). We repeat the experiments for unstable flow (see Fig. 6) and the same phenomena are observed. However, the viscous fingers are more pronounced.

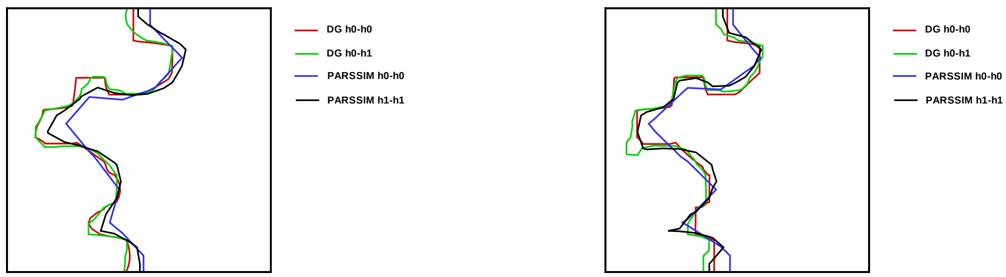

(a) (b)

Figure 3: Comparisons between DG and Parssim concentration isocontours for mobility ratio 10 and Peclet number (a) 40 and (b) 1600.

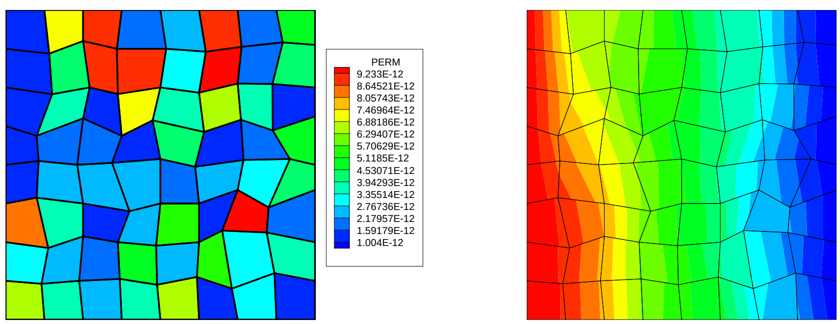

(a) (b)

Figure 4: (a) Permeability field on unstructured coarse mesh. (b) DG Pressure field on coarse unstructured mesh.

4. Conclusions

In this work, we have shown numerically that the DG method is well suited for fluid flow problems in porous media and in particular that it is competitive with other locally conservative methods for solving the miscible displacement problem. First, DG velocities are accurate enough so that coarser meshes can be used for solving the flow equation. Second, the DG method can capture the instabilities of the flow. Finally, the DG method can handle unstructured meshes in an easy and natural way.

REFERENCES

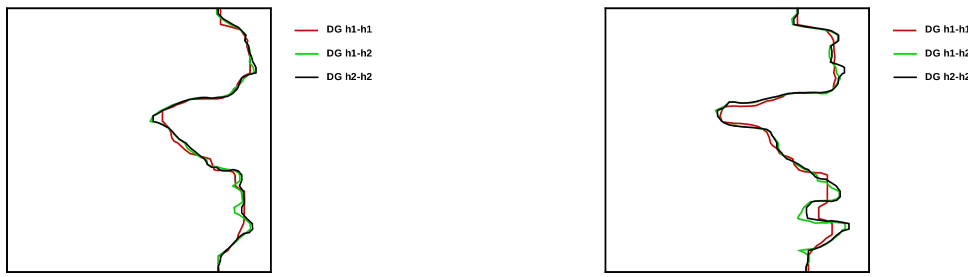

(a) (b)

Figure 5: Isocontours of the DG concentration for mobility ratio 1 and for Peclet number (a) 40 and (b) 1600.

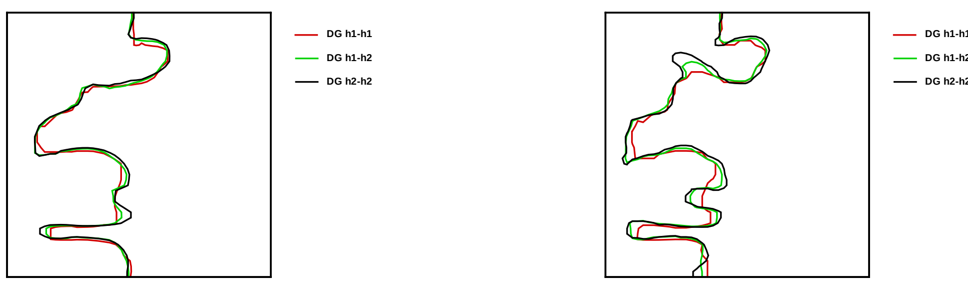

(a) (b)

Figure 6: Isocontours of the DG concentration for mobility ratio 10 and for Peclet number (a) 40 and (b) 1600.

1. Arbogast T. User's guide to Parssim1: the Parallel Subsurface Simulator, Single Phase. *Texas Institute for Computational and Applied Mathematics* 1998: **98-13**.
2. Cockburn B, Shu CW. The Runge-Kutta discontinuous Galerkin method for conservation laws V. *J. Comp. Physics* 1998; **141**:199–224.
3. Douglas J. The numerical simulation of miscible displacement in porous media. *Comp. Meth. in Nonlinear Mech.* 1980: 225–237.
4. Douglas J, Ewing RE, Wheeler MF. A time-discretization procedure for a mixed finite element approximation of miscible displacement in porous media. *R.A.I.R.O. Numerical Analysis* 1983; **17**(3):249–265.
5. Koval EJ. A method for predicting the performance of unstable miscible displacement in heterogeneous media *Soc. Pet. Eng. J.* 1963; **3**:145–154.
6. Rivière B, Wheeler MF, Girault V. A priori error estimates for finite element methods based on discontinuous approximation spaces for elliptic problems. *SIAM J. Numer. Anal.* 2001; **39**(3):902–931.

Prepared using cnmauth.cls